Original Research Article   Medicinal Chemistry

PHARMACOPHORE MODEL GENERATION & LIGAND BASED 3D-QSAR STUDY AND DESIGN OF NOVEL BIPHENYL DERIVATIVES OF BENZIMIDAZOLE AS ANTI-MYCOBACTERIAL AGENTS

SAZID ALI*[1], MOHD SHAHARYAR[2], SHAILENDRA SHARMA[1]

[1]Jodhpur institute of Pharmacy, Jodhpur National University,
Jodhpur, Rajasthan 342003, India
[2] School of Pharmaceutical Education and Research, Jamia Hamdard,
New Delhi 110062, India

ABSTRACT

With the aim of designing new chemical entities with enhanced inhibitory potencies against *Mycobacterium tuberculosis*, the 3D-QSAR studies were carried out on biphenyl analogues of the tuberculosis drug, (6S)-2-nitro-6-{[4-trifluoromethoxy)benzyl]oxy}-6, 7-dihydro-5H-imidazo[2,1-b][1,3]oxazine (PA-824), as presented here. The 3D-QSAR studies involve analysis of the quantitative relationship between the biological activity of a set of compounds and their three-dimensional structural properties, using statistical correlation methods. Anti-mycobacterial activity (MABA) was considered for the 3D-QSAR studies using the pharmacophore modelling. The hypothesis model results were found statistically significant ($q^2 > 0.7$ and $r^2 > 0.8$). Based on the findings of the 3D-QSAR model and structural insights, a series of new biphenyl derivatives of benzimidazole were designed and the anti-mycobacterial activities of the designed compounds were predicted. The analysis of pharmacophore generated has provided many clues about the structural requirement for the observed biological activity which shows that the electron-withdrawing groups at the terminal aryl rings are favorable for MABA inhibitory activity i.e., the addition of electron-withdrawing groups at this site will lead to increased MABA inhibition To add further, the OH, NH_2 and $CONH_2Ph$ groups should be avoided at para position and lipophilicity is significant factor for further improvement.

SAZID ALI*
Jodhpur institute of Pharmacy, Jodhpur National University,
Jodhpur, Rajasthan 342003, India

INTRODUCTION

Tuberculosis (TB), caused by *Mycobacterium tuberculosis* (*Mtb*), is still one of the world's deadly disease with crucial impact on medical and economic conditions of patients. In present TB treatment, a combination of two or more drugs like isoniazid, rifampicin, pyrazinamide, and Ethambutol is used to cure the patient. Today the difficulties faced in managing TB are due to, the long duration treatment regimens, the emergence of drug resistant *Mtb* strains and coinfection with HIV/AIDS. To overcome these, efforts are on for (a) development of long-acting drugs with extended-intervals of dosing in order to facilitate "Directly Observed Treatment Short course (DOTS)" and enhanced patient compliance, (b) prevention of MDR-TB strains by using drugs, which exhibit potent early microbicidal microbiocidal activity and (c) eradication of slowly metabolizing and, if possible, dormant *Mtb* population that cause relapse, using new classes of anti-TB drugs [1]. However, with rise of multi-drug resistant strains of *Mtb* there is urgent need to design new potent efficient inhibitors[2] or modifying the existing drugs to inhibit *Mtb* as well as pre-existing resistant variants due to occurrence of mutations during ongoing bacterial replication[3].
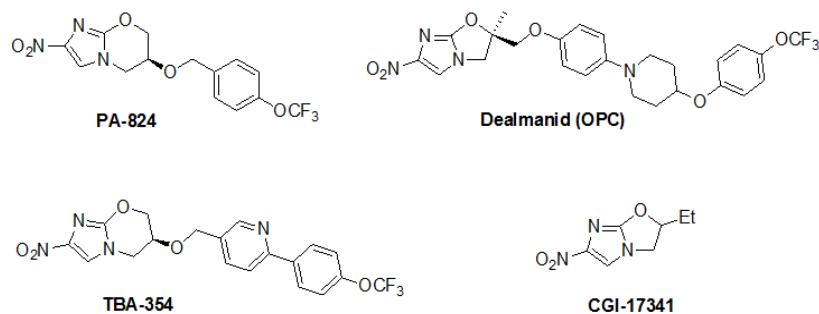

Figure 1
Structures of nitroimidazole based antitubercular agents

Three-dimensional Quantitative Structure-Activity Relationship (3D-QSAR) approach is one of the most powerful techniques which come in the class of ligand-based drug design where 3D structure of the target protein is unavailable. Thus, lead optimization with or without receptor 3D structure are the most important applications of 3D-QSAR[4]. The 3D-QSAR studies involve analysis of the quantitative relationship between the biological activity of a set of compounds and their three-dimensional structural properties, using statistical correlation methods. It allows 3D visual analysis for spatial arrangement of structural features with biological activity thus is advantageous over 2D-QSAR where model data has to be taken into consideration. In another 3D-QSAR CoMFA study on biphenyl analogues of the tuberculosis drug, (6S)-2- nitro-6-{[4-trifluoromethoxy)benzyl]oxy}-6,7-dihydro-5Himidazo[2,1-b][1,3]oxazine (PA-824) was carried out to design new chemical entities with enhanced inhibitory potencies against Mycobacterium tuberculosis[5]. Further a statistically significant model was established using CoMSIA and modelled Inhibitory activities of monocyclic nitroimidazoles against *Mycobacterium* using docking, pharmacophore alignment and comparative molecular similarity indices analysis (CoMSIA) methods[6]. A 3D-quantitative structure–activity relationship (QSAR) study on biphenyl analogues of the tuberculosis (TB) drug, PA-824 was performed using the comparative molecular field analysis (CoMFA) and comparative molecular similarity indices analysis (CoMSIA) approaches revealing that both the CoMFA and CoMSIA models possess high accommodating capacities and they would be reliable for predicting the pMIC values of new PA-824 derivatives Based on the models and structural insights, a series of new PA-824 derivatives was were designed and the anti-mycobacterial activities of the designed compounds were predicted based on the best 3D-QSAR model[7].

Table 1
Score of different parameters of the hypothesis AARR.325

S.No.	Parameters	Scores
1	Survival	288.49
2	Survival -inactive	285.773
3	Post-hoc	3.697
4	Site	0.99
5	Vector	0.908
6	Volume	0.797
7	Selectivity	0
8	Matches	57
9	Energy	0.986
10	Activity	8.824
11	Inactive	2.717

Related to the foregoing studies we are reporting 3D QSAR models for replicating (anti-mycobacterial activity [MABA]) conditions which are having very good predictive capability of new PA-824. Further we designed a new series of biphenyl derivatives of benzimidazole and predicted their antitubercular MABA activities by using the best 3D QSAR model. This work revealed the relationships between the biological activity and the molecular properties of the PA824 derivatives, and provided useful information for guiding the design of novel anti-mycobacterial agents. Some nitroimidazole based antimycobacterial drugs are in clinical evaluation (Figure 1).
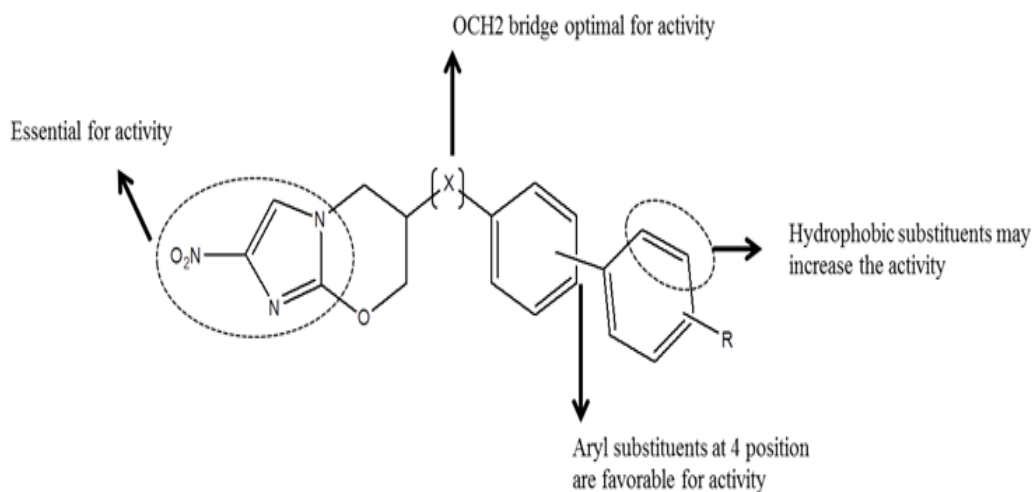

Figure 2
Design strategy for novel PA-824 derivatives

MATERIALS AND METHODS

Datasets
A large dataset of PA-824 analogues and experimental minimum inhibitory concentration (MIC) values were collected from the literatures (Denny et al., 2010). The quality of the biological data under investigation as well as the structural diversity of the dataset is the important foundations for success of QSAR studies. In this work, a series of 79 analogues of PA-824 was collected from published article. The *in vitro* MIC values employed in this work were measured under the same experimental conditions, a fundamental requirement for QSAR studies. The MIC values were converted into the corresponding pMIC values (Table 3) and used as dependent variables in the 3D-QSAR investigations. The MIC values of the molecules were expressed as micromolar (µM) units and converted to corresponding pMIC values according to the formula: pMIC = - log MIC.
The generation of consistent statistical models depends on the proper selection of both training and test sets in terms of structural diversity and property values distribution. The dataset consists of both active and inactive molecules, and the dataset was divided into training and test set using the "Automated Random Selection" option present in the PHASE software. 48 and 31 compounds were selected as training set and test set respectively (Table 3). The partitioning was so selected that there should be both active and inactive ligands in each test as well as training set. The dataset was then used for generating common pharmacophore hypotheses and subsequently for developing 3D-QSAR models (Figure 2, Table 3).

Computational details
PHASE-3.1 module of Maestro-9 (Phase3.1, Schrödinger, LLC, 2009) molecular modelling software was used to generate 3D pharmacophore models for the present series of compounds. The structures were sketched using maestro builder toolbar and were assigned as active and inactive by giving an appropriate activity threshold value (Tables 3). Sketched structures (Table 3) were prepared with the help of ligprep module and proper protonation states were assigned with the ionizer subprogram at pH = 7.2 ± 0.2 (LigPrep, Schrödinger, LLC, 2009). The conformations were generated with the help of MacroModel torsional sampling using OPLS_2005 force field (MacroModel, Schrödinger, LLC, 2009).
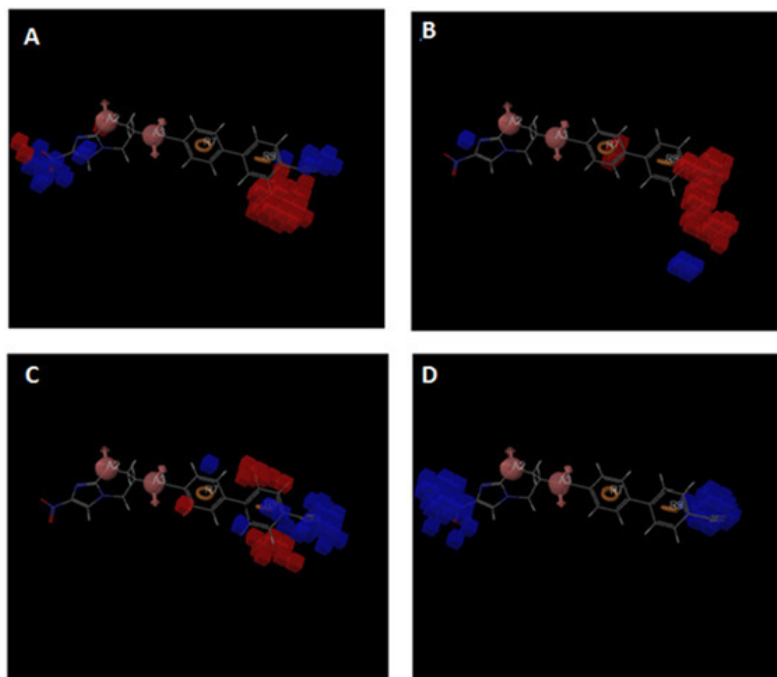
Figure 3
Atom-based 3D-QSAR model visualization for AARR.325 hypothesis in context of the most active inhibitor (compound 39) and various substituents effects: [A] electron-withdrawing feature, [B] hydrogen bond donor, [C] hydrophobic effects, and [D] negative ionic effect

Prepared ligands were then used for generating common pharmacophore hypothesis (CHPs) and QSAR models. As most ligands are flexible, it is, therefore, essential to consider a range of conformations to increase the chances of finding the most active conformer close to the bound structure; so it is necessary to generate all possible conformations. Accordingly, the prepared ligands were subjected to conformational analysis using confgen method implemented in the Schrödinger software. PHASE utilizes fine-grained conformational sampling and some scoring methods to identify CHPs for a series of molecules which have particular target specificity. Each hypothesis conveys a particular 3D conformation of a set of ligands in which the ligands are going to bind to the receptor. The best hypothesis was then correlated with known biological activity values to generate a 3D-QSAR model which identifies the whole structural features of molecules that govern activity[8-9].

Table 2
3D-QSAR statistical parameters

PLS Factor	SD	r^2	F	P	RMSE	q^2	Pearson-R
1	0.3727	0.4377	35.8	3.062e-007	0.5624	0.8528	0.7301
2	0.3089	0.6221	37	3.1e-010	0.5393	0.8616	0.7645
3	0.2385	0.7797	51.9	1.684e-014	0.5112	0.8676	0.8778
4	0.1844	0.8713	72.8	1.422e-018	0.4875	0.8717	0.9127
5	0.145	0.9223	99.6	3.56e-022	0.4795	0.8759	0.9376

Active analogue approach was used to identify a CPH which has been applied in generating significant 3D-QSAR models[10-12]. The common pharmacophores were culled from the conformations of the set of active ligands using a tree-based partitioning technique which groups together similar pharmacophores according to their inter-site distances. A tree depth of five with initial box size of 25.6 A° and final box size of 0.8 A° was used (Phase3.1, Schrödinger 2009; Samantha et al., 2008). Following which pharmacophores were scored and ranked. Scoring algorithm includes contributions from the alignment of site points and vectors, volume overlap, selectivity, number of ligands matched, relative conformational energy, and activity (Dixon et al., 2006). The selected AARR.325 hypothesis with various scores is reviewed in Table 1.The best pharmacophore hypothesis AARR.325 selected was used for further QSAR development. The mentioned 3D pharmacophore hypothesis in Figure 3 includes the following features: two hydrogen bond acceptor (A) in pink colour and two aromatic rings (R) in yellow colour. The 2D representation of the AARR.325 hypothesis is given in Figure 2.

Table 3
Fitness and PHASE predicted activity data for AARR.325 hypothesis

Ligand Name	QSAR Set	R	IC50	pIC50	Predicted Activity pIC50	Pharm Set	Fitness
1.	training	H	0.045	1.346787	1.263	active	2.96
2.	training	2-CF$_3$	0.077	1.113509	1.212	active	2.69
3.	test	2-CHO	0.08	1.09691	1.091	active	2.74
4.	training	2-F	0.19	0.721246	1.156	inactive	2.87
5.	test	2-Cl	0.15	0.823909	0.989	active	2.81
6.	training	2-OH	0.12	0.920819	1.028	active	2.85
7.	training	2-OMe	0.065	1.187087	1.364	active	2.82
8.	test	2-OEt	0.03	1.522879	1.497	active	2.79
9.	training	2-O(CH$_2$)$_3$OH	0.34	0.468521	0.723	inactive	2.75
10.	test	2-OCF$_3$	0.035	1.455932	1.324	active	2.74
11.	training	2-OPh	0.06	1.221849	1.212	active	2.72
12.	training	2-SMe	0.087	1.060481	1.124	active	2.74
13.	training	3-iPr	0.14	0.853872	0.987	active	2.27
14.	test	3-Ph	0.31	0.508638	0.682	inactive	2.79
15.	training	3-CF$_3$	0.067	1.173925	1.126	active	2.26
16.	training	3-CHO	0.14	0.853872	0.926	active	2.89
17.	training	3-CN	0.12	0.920819	0.915	active	2.62
18.	training	3-CONH$_2$	2.8	-0.44716	-0.368	inactive	2.28
19.	training	3-F	0.045	1.346787	1.142	active	2.89
20.	training	3-Cl	0.06	1.221849	1.386	active	2.6
21.	test	3-OH	0.14	0.853872	0.626	active	2.89
22.	training	3-OMe	0.27	0.568636	0.538	inactive	2.9
23.	training	3-O(CH$_2$)$_2$OH	0.46	0.337242	0.286	inactive	2.84
24.	training	3- O(CH$_2$)$_3$OH	0.18	0.744727	0.973	inactive	2.51
25.	training	3- O(CH$_2$)$_2$NMe2	1.5	-0.17609	-0.154	inactive	2.49
26.	test	3-OCF$_3$	0.077	1.113509	1.047	active	2.8
27.	test	3-OCH$_2$Ph	0.12	0.920819	1.023	active	2.47
28.	training	3-SMe	0.077	1.113509	1.056	active	2.87
29.	training	3-NH$_2$	0.12	0.920819	0.893	active	2.61
30.	training	3-NO$_2$	0.13	0.886057	0.859	active	2.87
31.	test	4-iPr	0.1	1.000000	0.943	active	2.61
32.	training	4-tBu	0.095	1.022276	1.129	active	2.58
33.	test	4-Ph	0.09	1.045757	1.034	active	2.86
34.	training	4-CF$_3$	0.03	1.522879	1.483	active	2.89
35.	training	4-CH$_2$OH	0.54	0.267606	0.097	inactive	2.94
36.	test	4-CH$_2$OtBu	0.077	1.113509	0.952	active	2.82
37.	training	4-CH$_2$NHPh	0.06	1.221849	1.152	active	2.51
38.	test	4-CHO	0.2	0.69897	0.738	inactive	2.93
39.	training	4-CN	0.025	1.60206	1.564	active	2.22
40.	test	4-CONH$_2$	2.1	-0.32222	-0.283	inactive	2.33
41.	training	4-COMe	0.04	1.39794	1.458	active	2.62
42.	training	4-F	0.015	1.823909	1.758	active	2.95
43.	test	4-Cl	0.015	1.823909	1.562	active	3
44.	training	4-OH	0.64	0.19382	0.149	inactive	2.67
45.	test	4-OMe	0.065	1.187087	1.230	active	2.94
46.	test	4-OiPr	0.25	0.60206	0.502	inactive	2.88
47.	training	4-OPh	0.04	1.39794	1.351	active	2.55
48.	test	4-O(CH$_2$)$_2$OH	0.55	0.259637	0.248	inactive	2.89
49.	test	4- O(CH$_2$)$_3$OH	0.6	0.221849	0.317	inactive	2.86
50.	training	4-O(CH$_2$)$_3$ Nmorpholine	0.097	1.013228	1.142	active	2.46
51.	training	4-OCF$_2$H	0.05	1.30103	1.426	active	2.89
52.	training	4-OCF$_3$	0.035	1.455932	1.437	active	2.84
53.	training	4-SMe	0.075	1.124939	1.119	active	2.61
54.	test	4-SO$_2$Me	0.067	1.173925	1.211	active	2.56
55.	training	4-NH$_2$	0.49	0.309804	0.362	inactive	2.93
56.	training	2-CL,4-CF$_3$	0.03	1.522879	0.963	active	2.78
57.	test	2-Cl,4-OCF$_3$	0.04	1.39794	1.120	active	2.76
58.	test	2-Cl,6-OMe	0.055	1.259637	1.173	active	2.58
59.	test	2-F,4-OCF$_3$	0.045	1.346787	1.428	active	2.53
60.	test	2-F,6-OMe	0.13	0.886057	0.729	active	2.79
61.	test	2,6-diMe	0.39	0.408935	0.218	inactive	2.68
62.	training	2,6-diOMe	0.31	0.508638	0.562	inactive	2.51
63.	test	3,4-diF	0.03	1.522879	1.439	active	2.64
64.	test	3-Cl,4-CF$_3$	0.06	1.221849	1.382	active	2.57
65.	training	3-Cl,4-OCF$_3$	0.03	1.522879	1.729	active	2.27
66.	training	3-OCF$_3$,4-Cl	0.04	1.39794	1.257	active	2.83
67.	test	3-CF$_3$,4-Cl	0.035	1.455932	1.226	active	2.52
68.	training	3-NO$_2$,4-OCF$_3$	0.045	1.346787	1.384	active	2.79
69.	test	3-F,4-OMe	0.04	1.39794	1.318	active	2.62
70.	training	3-F,4-OCF$_3$	0.03	1.522879	1.639	active	2.84
71.	training	3-OMe,4-F	0.045	1.346787	1.259	active	2.91
72.	test	3-OCF$_2$H,4-Cl	0.03	1.522879	1.384	active	2.56

73.	training	3-OH,4-Cl	0.2	0.69897	0.538	inactive	2.92
74.	test	3,5-diOMe	0.28	0.552842	0.382	inactive	2.52
75.	training	2-OMe,3,5-diF	0.04	1.39794	1.183	active	2.77
76.	training	2,6-diMe,4-OMe	0.58	0.236572	0.273	inactive	2.69
77.	training	3,4,5-triF	0.04	1.39794	1.429	active	2.6
78.	training	3,5-diMe,4-OH	0.3	0.522879	0.547	inactive	2.59
79.	test	3,5-diF,4-OMe	0.045	1.346787	1.293	active	2.88

Building of QSAR model

AARR.325 hypothesis was used to generate a robust 3D-QSAR model. Random selection was done for obtaining training and test partition for model generation. PHASE has two 3D structure alignment tools: the atom-based alignment and the pharmacophore- based alignment. Atom-based alignment technique is good for the structures which contains a relatively small number of rotatable bonds and some common structural framework. This alignment technique has been used for generating number of 3D-QSAR models for diversity of structures (Viney et al, 2008; Dixon et al, 2006). QSAR model was built by atom-based selection criterion. Statistical significance of various models is given in Table 2. The pharmacophore-based QSAR does not consider possible steric clashes with the receptor while atom-based QSAR considers all possible steric clashes with the receptor and uses the entire molecular structure for generating QSAR models. Therefore, an atom-based QSAR model is more useful in explaining the structure-activity relationship[13]. In atom-based QSAR, a molecule is treated as a set of overlapping van der Waal spheres in which each atoms (and hence each sphere) are classified in six categories according to a simple set of rules:

i) Hydrogen bond donors (D): Hydrogens attached to polar atoms.
ii) Hydrophobic/non-polar (H) : Carbons, halogens and C–H hydrogens.
iii) Negative ionic (N) : Atoms with an explicit negative ionic charge.
iv) Positive ionic (P) : Atoms with an explicit positive ionic charge.
v) Electron-withdrawing (W) : Non-ionic atoms.
vi) miscellaneous (X) : All other types of atoms

To develop the QSAR model, van der Waals models of the aligned training set molecules were placed in a regular grid of cubes, with each cube allotted zero or more "bits" to account for different types of atoms in the training set that occupy the cube. This representation gives rise to binary valued occupation patterns that can be used as independent variables to create partial least-squares (PLS) QSAR models[14]. Atom-based QSAR models were generated for the selected hypothesis using the training set compounds with the help of a grid spacing of 1.0 A°. The best QSAR models were validated by predictive activities of the test set compounds. A model with four and three PLS factors were considered as the best statistical models for the enzymatic and cellular inhibitory activities, respectively. The maximum number of PLS factors in each model can be 1/5 the total number of training set molecules since further increase in the number of PLS factors did improve the model statistics or predictive ability.

RESULTS AND DISCUSSION

A 3D-QSAR study was successfully performed on the series of biphenyl derivatives of benzimidazole to understand the effect of spatial arrangement of structural features on anti-mycobacterium activities (MABA). Results of the 3D-QSAR are presented in Figure 3. The blue cubes of the 3D pharmacophore regions refer to ligand regions in which the specific feature is vital for activity, whereas the red cubes demonstrate that particular structural feature or functional group is not essential for the activity or likely a reason for decreased binding potential.

Table 4
Some anti-tubercular molecules designed with
3D QSAR model with their predicted activities

I

II

III

IV
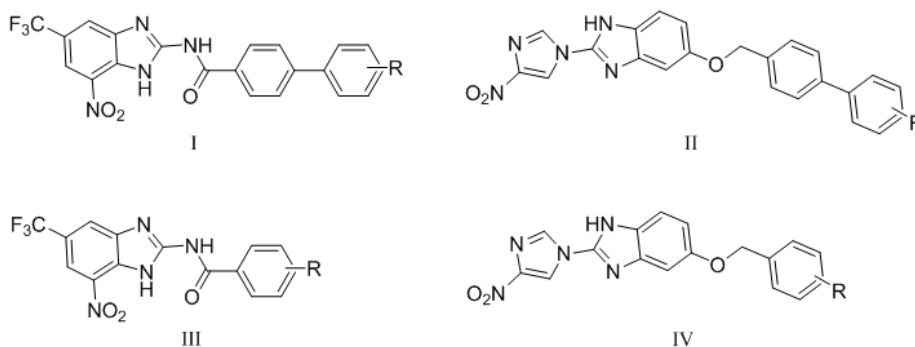
S.No.	Compound	X	R	Predicted Activity pIC50
			FOR STRUCTURE-I	
1.	S1	NHCO	4-OH	0.007446
2.	S2	NHCO	4-OMe	1.376751
3.	S3	NHCO	4-CF$_3$	1.283997

No.	Code	Group	Substituent	Value
4.	S4	NHCO	4-SMe	1.124939
5.	S5	NHCO	4-NH$_2$	-0.05308
6.	S6	NHCO	4-OCF$_3$	1.19382
7.	S7	NHCO	4-CONH$_2$	-0.19396
8.	S8	NHCO	4-CONHPh	1.187087
9.	S9	NHCO	4-SO$_2$Me	0.099633
10.	S10	NHCO	4-CN	1.346787
11.	S11	NHCO	4-COMe	1.148742
12.	S12	NHCO	4-NHSO$_2$Me	-0.35083
13.	S13	NHCO	4-Nmorpholine	-0.69478
14.	S14	NHCO	2-Me,4-F	1.060481
15.	S15	NHCO	2-Me,4-CF$_3$	0.754487
16.	S16	NHCO	2-Me,4-CN	0.779892
17.	S17	NHCO	2-Me,4-OMe	0.777284
18.	S18	NHCO	2-Me,4-OCF$_3$	0.943095
19.	S19	NHCO	2-iPr,4-F	0.844664
20.	S20	NHCO	2-iPr,4-CF$_3$	0.90309
21.	S21	NHCO	2-iPr,4-CN	1.031517
22.	S22	NHCO	2-iPr,4-OMe	1.008774
23.	S23	NHCO	2-iPr,4-OCF$_3$	-0.086
24.	S24	NHCO	3-F,4-F	-0.13354
25.	S25	NHCO	3-F,4-CF$_3$	1.481486
26.	S26	NHCO	3-F,4-CN	1.173925
27.	S27	NHCO	3-F,4-OMe	1.431798
28.	S28	NHCO	3-F,4-OCF$_3$	1.49485
29.	S29	SCH$_2$	4-F	-0.59028
30.	S30	SCH$_2$	4-CF$_3$	-0.50987
31.	S31	SCH$_2$	4-CN	-0.54876
32.	S32	SCH$_2$	4-OMe	-0.5027
33.	S33	SCH$_2$	4-OCF$_3$	-0.47451
34.	S34	NHCH$_2$	4-F	-0.4553
35.	S35	NHCH$_2$	4-CF$_3$	-0.43823
36.	S36	NHCH$_2$	4-CN	-0.39602
37.	S37	NHCH$_2$	4-OMe	-0.31408
38.	S38	NHCH$_2$	4-OCF$_3$	-0.29579
39.	S39	OCH$_2$	4-F	-0.0976
40.	S40	OCH$_2$	4-CF$_3$	-0.05269
41.	S41	OCH$_2$	4-CN	0.049149
42.	S42	OCH$_2$	4-OMe	0.126098
43.	S43	OCH$_2$	4-OCF$_3$	0.187755
		FOR STRUCTURE-II		
44.	S44	NHCO	4-F	-0.25091
45.	S45	NHCO	4-CF$_3$	-0.2927
46.	S46	NHCO	4-CN	-0.24527
47.	S47	NHCO	4-OMe	-0.23578
48.	S48	NHCO	4-OCF$_3$	-0.08493
49.	S49	SCH$_2$	4-F	-0.52401
50.	S50	SCH$_2$	4-CF$_3$	-0.59824
51.	S51	SCH$_2$	4-CN	-0.62459
52.	S52	SCH$_2$	4-OMe	-0.65571
53.	S53	SCH$_2$	4-OCF$_3$	-0.44451
54.	S54	NHCH$_2$	4-F	-0.40432
55.	S55	NHCH$_2$	4-CF$_3$	0.012334
56.	S56	NHCH$_2$	4-CN	-0.52789
57.	S57	NHCH$_2$	4-OMe	-0.38596
58.	S58	NHCH$_2$	4-OCF$_3$	-0.46195
59.	S59	OCH$_2$	4-F	1.142668
60.	S60	OCH$_2$	4-CF$_3$	1.21467
61.	S61	OCH$_2$	4-CN	1.49485
62.	S62	OCH$_2$	4-OMe	1.283997
63.	S63	OCH$_2$	4-OCF$_3$	1.19382
64.	S64	OCH$_2$	3-F,4-F	0.906578
65.	S65	OCH$_2$	3-F,4-CF$_3$	1.408935
66.	S66	OCH$_2$	3-F,4-CN	1.251812
67.	S67	OCH$_2$	3-F,4-OMe	1.552842
68.	S68	OCH$_2$	3-F,4-OCF$_3$	1.455932
		FOR STRUCTURE-III		
69.	S69	NHCO	4-F	-0.08458
70.	S70	NHCO	4-CF$_3$	0.133713
71.	S71	NHCO	4-CN	0.66354
72.	S72	NHCO	4-OMe	1.031517
73.	S73	NHCO	4-OCF$_3$	1.004365
74.	S74	NHCO	4-Nmorpholine	-0.37051
75.	S75	NHCO	4-Nthiomorpholine	-0.5858
76.	S76	NHCO	4-NHSO$_2$Me	-0.05154
77.	S77	NHCO	3-F,4-F	0.136083
78.	S78	NHCO	3-F,4-CF$_3$	0.567031
79.	S79	NHCO	3-F,4-CN	0.790485

80.	S80	NHCO	3-F,4-OMe	0.140261
81.	S81	NHCO	3-F,4-OCF$_3$	0.939302
FOR STRUCTURE-IV				
82.	S82	OCH$_2$	4-F	1.207608
83.	S83	OCH$_2$	4-CF$_3$	1.481486
84.	S84	OCH$_2$	4-CN	1.537602
85.	S85	OCH$_2$	4-OMe	1.259637
86.	S86	OCH$_2$	4-OCF$_3$	1.207608
87.	S87	OCH$_2$	4-Nmorpholine	-0.25091
88.	S88	OCH$_2$	4-Nthiomorpholine	-0.2971
89	S89	OCH$_2$	4-NHSO$_2$Me	-0.1209
90.	S90	OCH$_2$	3-F 4-F	-0.06221
91.	S91	OCH$_2$	3-F,4-CF$_3$	1.142668
92.	S92	OCH$_2$	3-F,4-CN	1.236572
93.	S93	OCH$_2$	3-F,4-OMe	1.200659
94.	S94	OCH$_2$	3-F,4-OCF$_3$	1.148742

The reliability of the present 3D-QSAR analyses can be justified by the fact that all statistical measures are at significant level. Ninety-nine percentage variance of the model signifies agreement between the observed and predicted activity. The fitness graph is presented in Figure 4. Observed and predicted activity data are summarized in Table 3. Validity of the model can be expressed by internal predictivity (q2 = 0.8759), which is obtained by leave one out (LOO) method. Higher value of F (99.6) is indicative of statistically significant regression model, which is supported by the small value of the variance ratio (P), an indication of a high degree of confidence. Lesser values of standard deviation for the regression (0.145) and RMSE (0.4795) further make an implication that the data used for model generation is best for the QSAR analysis. Apart from the above-mentioned features, PLS factor also confirms the reliability of the model. In the present study PLS factor was taken as 5 and for each increment it gives one equation. In addition to the above parameters it is interesting to note that active ligands are closely fitted to the regression line and inactive ligands are scattered. 3D-pharmacophore regions around compounds are shown in Figure 3. Blue and red cubes represent favorable and unfavorable regions respectively, for the selected pharmacophore. Figure 3A represents electron-withdrawing characteristic for the AARR.325 hypothesis. Visual analysis of the Figure 3A demonstrates the throng of the blue cubes around aryl ring site suggesting that electron-withdrawing groups are favorable for MABA inhibitory activity i.e., the addition of electron-withdrawing groups at this site will lead to increased MABA inhibition like compounds S2, S3. Figure 3B illustrates H-donor characteristics of the hypothesis. Red cubes near the ring B of biphenyl side chain suggests that addition of hydrogen bond donor groups (NH$_2$, OH, CONH$_2$) will lead to poor binding to the receptor (compound S1, S5 and S7). It is interesting to note here that some of the blue cubes are also present near imidazole ring which shows that free NH group in the imidazole ring is also favorable. Figure 3C demonstrates the effect of positive and negative hydrophobic potential. Hydrophobic groups are well tolerated at the extreme end of biphenyl side chain (S2, S3 and S6), while hydrophilic groups are not favorable (S9, S12 and S13). Also Figure 3D shows negative ionic groups at the terminals are favorable for the inhibitory activity.
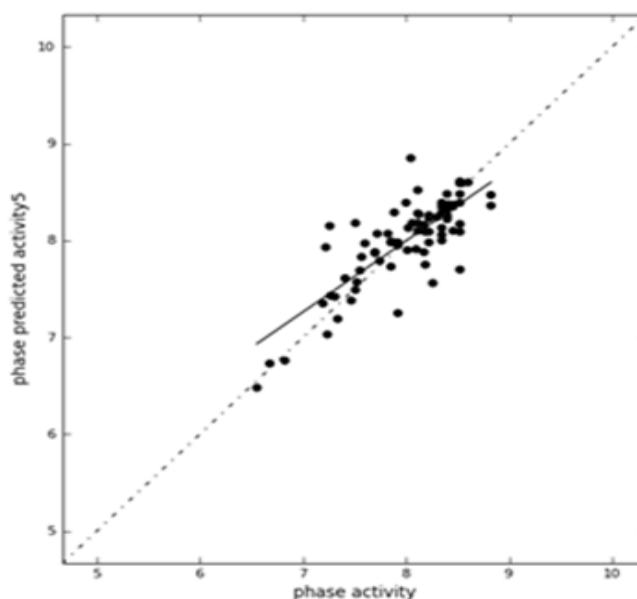

Figure 4
*Fitness Graph between observed activity versus predicted activity
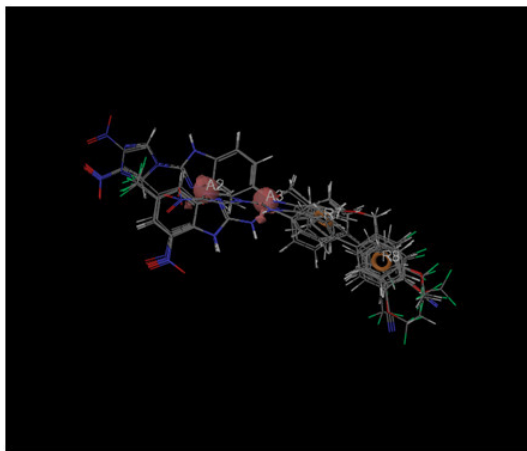for training and test set compound for AARR.325 hypothesis*

Figure 5
Alignment of ligands to the pharmacophore

Table 4 shows a comparison of all of the NHCO, SCH$_2$, NHCH$_2$ and OCH$_2$-linked analogues of structure I and structure II bearing the same substituents on the terminal ring. The SAR studies reveal that NHCO and OCH$_2$ bridge is optimal for greater activity for analogues of structure I and structure II respectively. This is demonstrated that single aryl ring analogues bearing the same substituents on the terminal ring are notably poor while some analogues retain activity in case of S83, S84. The active alignment of the dataset is presented in Figure 5.

CONCLUSION

The pharmacophore based 3D QSAR analysis using 79 PA-824 derivatives was used to build statistically robust hypothesis model with good correlative and predictive capability of anti-TB activity. The 3D-QSAR model discussed above explains how electron withdrawing, hydrophobic, and H-donor properties should be modified to achieve better anti-TB activity. The hypothesis model results were statistically significant ($q^2 > 0.7$ and $r^2 > 0.8$). The q^2, r^2, and other parameter values are in an acceptable criterion for statistical validity and allow for the assumption of a significant QSAR model. The analysis of pharmacophore generated has provided many clues about the structural requirement for the observed biological activity. To add further, the OH, NH$_2$ and CONH$_2$Ph groups should be avoided at para position and lipophilicity is significant factor for further improvement. Based on pharmacophore model and structural insights, a series of new biphenyl analogues of benzimidazole were designed and the anti-mycobacterial activities of the designed compounds were predicted based on the best 3D-QSAR model. Compounds with best predicted activity will be synthesized and evaluated in laboratory for their anti-mycobacterial activity. This analysis could be help in the rational design of potential drug candidates with an enhanced inhibitory potency.

CONFLICT OF INTEREST

Conflict of interest declared none.

REFERENCES

1. Gwynn MN, Portnoy A, Rittenhouse SF, Payne DJ. Challenges of antibacterial discovery revisited. Ann N Y Acad Sci 2010; 1213: 5-19.
2. (a) Hadda TB, Bennani B, Kerbal A, Daoudi M, Filali Baba B, Houari GA, et al. Combined drug design of potential Mycobacterium tuberculosis and HIV-1 inhibitors: 3',4'-di-substituted-4'H-spiro [isothiochromene-3,5'-isoxazol]-4(1H)-one. ARKIVOC 2007; 16:19–40. (b) Unissa AN, Hassan S, Selvakumar N. Elucidating isoniazid resistance in mycobacterium tuberculosis using molecular docking approach. Int J Pharma. Bio. Sci. 2012; 3(1):B314-6.
3. Denny WA, Palmer BD, Thompson AM, Sutherland HS, Blaser A, Kmentova I, et al. Synthesis and structure-activity studies of biphenyl analogues of the tuberculosis drug (6S)-2-nitro-6-{[4-(trifluoromethoxy) benzyl] oxy}-6, 7-dihydro-5H-imidazo [2, 1-b][1,3] oxazine (PA-824). J Med Chem 2010; 53:282–4.
4. Pasha FA, Srivastava HK, Beg Y, Singh PP. DFT based electrophilicity index and QSAR study of phenols as anti-Leukaemia agent American. J Immunol 2006; 2(1):23–8.
5. Masand VH, Patil KN, Nazerruddin GM, Jawarkar RD, Bajaj SO. QSAR and CoMFA studies of biphenyl analogs of the anti-tuberculosis drug

(6S)-2-nitro-6-{[4-   (trifluoromethoxy)benzyl]oxy}-6,7-dihydro-5H-imidazo [2,1-b][1,3] oxazine (PA-824). Med Chem Res 2012; 21:2624–9.

6. Lee SH, Choi M, Kim P, Myung PK. 3D-QSAR and Cell Wall Permeability of Antitubercular Nitroimidazoles against Mycobacterium tuberculosis. Molecules 2013; 18:13870-85.

7. Inturi B, Pujar GV, Purohit MN. Structural insights of PA-824 derivatives: ligand-based 3D-QSAR study and design of novel PA824 derivatives as anti-tubercular agents. J Recept Signal Transduct Res 2015; early online: 1-11.

8. Anna MA, Tutone M, Lauria A. 3D-QSAR pharmacophore modelling and in silico screening of new Bcl-xl inhibitors. Eur J Med Chem 2010; 45:4774–82.

9. Samantha L, Cesare M, Aleksey K, Mattia S, Stefano M, Elena C, et al. SAR and QSAR study on 2-aminothiazole derivatives, modulators of transcriptional repression in Huntington's disease. Bioorg Med Chem 2008; 16:5695–703.

10. Sachin SN, Mariam SD. Pharmacophore refinement and 3DQSAR studies of histamine H3 antagonists. QSAR Comb Sci 2007; 26:744–53.

11. Viney L, Rajendra K, Jagmohan SS, Rajendra K, Narasingapuram AK, Vitukudi NB. QSAR models for prediction of glycogen synthase kinase-3b inhibitory activity of indirubin derivatives. QSAR Comb Sci 2008; 27:718–28.

12. Dixon SL, Smondyrev AM, Knoll EH, Rao SN, Shaw DE, Friesner RA. PHASE: a new engine for pharmacophore perception, 3D QSAR model development, and 3D database screening: 1. Methodology and preliminary results. J Comput Aided Mol Des 2006; 20:647–71.

13. Shah UA, Deokar HS, Kadam SS, Kulkarni VM. Pharmacophore generation and atom-based 3D-QSAR of novel 2-(4- methylsulfonylphenyl) pyrimidines as COX-2 inhibitors. Mol Divers 2010; 14:559–68.

14. Kathiravan MK, Khilare MM, Chothe AS, Nagras MA. Design and development of topoisomerase inhibitors using molecular modelling studies. J Chem Biol. 2013 Jan; 6(1): 25–36.

Reviewer of this Article

Stanley E. UKWUEZE

Faculty of Pharmaceutical Sciences, University of
Port Harcourt [UNIPORT], Choba, Rivers State,
Nigeria.

Dr. Ravinesh Mishra

Associate Professor,
School of Pharmacy and Emerging Science,
Baddi University of Emerging and Technology,
Baddi, Himachal Pradesh - 173205, India.

Prof.Dr.Prapurna Chandra Rao

Assistant Proffessor, KLE University,
Belgaum, Karnataka, India.

Prof.Dr.K.Suriaprabha

Asst. Editor , International Journal
of Pharma and Bio sciences.

Prof.P.Muthuprasanna

Managing Editor , International
Journal of Pharma and Bio sciences.

We sincerely thank the above reviewers for peer reviewing the manuscript